[CANCER RESEARCH 61, 6649–6655, September 15, 2001]

Advances in Brief

Cell Surface Tumor Endothelial Markers Are Conserved in Mice and Humans[1]

Eleanor B. Carson-Walter, D. Neil Watkins, Akash Nanda, Bert Vogelstein, Kenneth W. Kinzler,[2] and Brad St. Croix[2]

The Howard Hughes Medical Institute [E. B. C-W., B. V.] and The Johns Hopkins Oncology Center [D. N. W., A. N., K. W. K., B. S. C.], Baltimore, Maryland 21231

Abstract

We recently identified genes encoding tumor endothelial markers (*TEM*s) that displayed elevated expression during tumor angiogenesis. From both biological and clinical points of view, *TEM*s associated with the cell surface membrane are of particular interest. Accordingly, we have further characterized four such genes, *TEM1*, *TEM5*, *TEM7*, and *TEM8*, all of which contain putative transmembrane domains. TEM5 appears to be a seven-pass transmembrane receptor, whereas TEM1, TEM7, and TEM8 span the membrane once. We identified mouse counterparts of each of these genes, designated *mTEM1*, *mTEM5*, *mTEM7*, and *mTEM8*. Examination of these *mTEM*s in mouse tumors, embryos, and adult tissues demonstrated that three of them (*mTEM1*, *mTEM5*, and *mTEM8*) were abundantly expressed in tumor vessels as well as in the vasculature of the developing embryo. Importantly, expression of these *mTEM*s in normal adult mouse tissues was either undetectable or detected only in a small fraction of the vessels. These results demonstrate conservation of human and mouse tumor angiogenesis at the molecular level and support the idea that tumor angiogenesis largely reflects normal physiological neovascularization. The coordinate expression of *TEM1*, *TEM5*, and *TEM8* on tumor endothelium in humans and mice makes these genes attractive targets for the development of antiangiogenic therapies.

Introduction

Inhibition of tumor angiogenesis as an anticancer strategy has generated much excitement among cancer researchers and clinicians. This enthusiasm stems from several theoretical advantages of targeting the endothelial cells that line tumor vessels rather than the tumor cells themselves (reviewed in Refs. 1 and 2): (*a*) targeting endothelial cells rather than tumor cells obviates many of the pharmacokinetic problems associated with drug delivery (3); (*b*) a significant bystander effect can also be expected because each endothelial cell supports the growth of many tumor cells; and (*c*) targeting the genetically stable endothelial cells should reduce the likelihood of developing resistant disease and should be applicable to a wide variety of tumor types (4, 5). However, realization of the full potential of antiangiogenic approaches will require a better understanding of the molecular differences between normal and tumor vessels, effective strategies to exploit these differences, and model systems in which to evaluate them.

To further understand human tumor angiogenesis, we recently conducted an unbiased gene expression analysis of endothelial cells isolated from normal human colonic tissue or from human colorectal cancers (6). This analysis identified 46 transcripts, named *TEM*s,[3] which were significantly up-regulated in tumor compared with normal endothelium. The majority of these genes had not been characterized previously. Expression of several of these *TEM*s in tumor endothelium was confirmed by reverse transcription-PCR and *in situ* hybridization. TEMs localized on the cell surface and conserved across species are of particular interest for future therapeutic approaches for two reasons: (*a*) cell surface targets are directly accessible via the bloodstream, facilitating detection as well as intervention with both small molecules and macromolecular compounds; and (*b*) conservation of such cell surface proteins allows the establishment of model systems that are required for preclinical development and testing. In this regard, rodent tumor models are the gold standard, but the extent of overlap between tumor angiogenesis in rodents and humans is unclear.

With these principles in mind, we set out to identify a series of cell surface *TEM*s that were structurally and functionally conserved in mouse and human tumor endothelium. To find such genes, we expanded the sequence of the most differentially expressed novel *TEM*s and used hydrophobicity plots to predict cell surface localization. We then identified and determined the sequence of the mouse counterparts of these genes and used *in situ* hybridization to examine mRNA expression patterns in murine tumors, embryos, and adult tissues. These studies identified three cell surface *TEM*s that had similar properties in both species and provide new evidence that angiogenesis in tumors is similar to normal developmental angiogenesis.

Materials and Methods

Identification of Human TEMs. Partial sequences were completed by performing 5′ RACE with the Marathon cDNA Amplification kit (Clontech, Palo Alto, CA) according to the manufacturer's protocol with Marathon-Ready cDNA from human fetal brain (Clontech) as a template. RACE products were sequenced using the Big Dye Terminator Cycle Sequencing Ready Reaction kit (Applied Biosystems, Foster City, CA) and analyzed in an ABI 3700 automated sequencer. Extending the EST sequences identified previously by the *TEM3* tag revealed this to be a longer version of the *TEM7* transcript, derived from a second polyadenylation site. *TEM7R* EST sequences were identified by homology to *TEM7* using tBLASTn of the National Center for Biotechnology Information database, and the complete sequence was identified using RACE.

Identification of Mouse TEMs. Mouse ESTs homologous to human *TEM1*, *TEM5*, *TEM7*, and *TEM8* were identified using BLASTn and tBLASTn searches. Extensive 5′ and 3′ RACE analysis was performed using the Marathon cDNA Amplification kit (Clontech) to identify the complete sequences. RACE was performed using mouse specific internal primers and Marathon-Ready cDNA prepared from a xenografted human lung cancer (Clontech).

Received 5/18/01; accepted 8/1/01.

The costs of publication of this article were defrayed in part by the payment of page charges. This article must therefore be hereby marked *advertisement* in accordance with 18 U.S.C. Section 1734 solely to indicate this fact.

[1] Supported by the Miracle Foundation and NIH Grants CA57345, CA62924, and Training Grant 5 T32 GM07309. D. N. W. is a C. J. Martin Fellow of the National Health and Medical Research Council of Australia. A. N. is a student in the Medical Scientist Training Program and the Program in Human Genetics. B. S. C. is a research Fellow of the National Cancer Institute of Canada supported with funds provided from the Terry Fox Run. K. W. K. received research funding from Genzyme Molecular Oncology (Genzyme). Under a licensing agreement between the Johns Hopkins University and Genzyme, the SAGE technology was licensed to Genzyme for commercial purposes, and B. V. and K. W. K. are entitled to a share of royalty received by the university from the sales of the licensed technology. The SAGE technology is freely available to academia for research purposes. B. S. C., B. V., and K. W. K. are consultants to Genzyme. The university and researchers (B. V. and K. W. K.) own Genzyme stock, which is subject to certain restrictions under university policy. The terms of these arrangements are being managed by the university in accordance with its conflict of interest policies.

[2] To whom requests for reprints should addressed, at The Johns Hopkins Oncology Center, 1650 Orleans Street, Room 588, Baltimore, MD 21231. Fax: (410) 955-0548; E-mail: kinzlke@jhmi.edu (K. W. K.) or stcroix@jhmi.edu (B. S. C.).

[3] The abbreviations used are: TEM, tumor endothelial marker; RACE, rapid amplification of cDNA ends; EST, expressed sequence tag; DIG, digoxigenin; VEGFR, vascular endothelial growth factor receptor; GPCR, G protein-coupled receptor; LRR, leucine-rich repeat; vWF, von Willebrand factor; SAGE, serial analysis of gene expression.

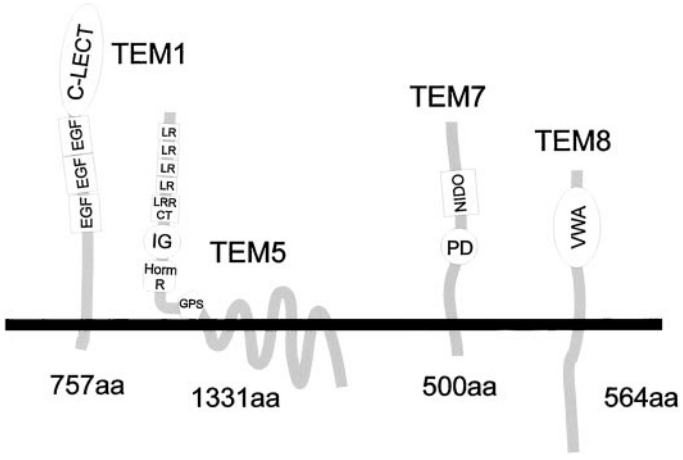

Fig. 1. Predicted structures of TEM1, TEM5, TEM7, and TEM8. Domain sizes are approximate. *C-LECT*, C-lectin like domain; *EGF*, epidermal growth factor-like domain; *LRR CT*, LRR COOH-terminal type; *IG*, immunoglobulin-like domain; *Horm R*, hormone receptor domain; *GPS*, GPCR proteolysis site; *NIDO*, nidogen-like domain; *PD*, plexin-like domain; *VWA*, von Willebrand A domain.

Bioinformatics. Amino acid alignments were performed using the ClustalW program (7). Hydrophobicity plots were created using DAS software (8). Signal peptides were determined using the SignalP program (9). Domain structures were found using SMART software (10) and Pfam software (11). Signaling sites were predicted using Scansite software (12).

***In Situ* Hybridization.** DIG-labeled antisense RNA probes were generated by PCR amplification of 500–600-bp products incorporating T7 promoters into the antisense primers. *In vitro* transcription was performed with DIG RNA labeling reagents and T7 RNA polymerase according to the manufacturer's instructions (Roche, Indianapolis, IN). Tumors and normal tissues were dissected, embedded in OCT, frozen in a dry ice-methanol bath, and cryosectioned at 7 μm. Embryos were prefixed in buffered 4% paraformaldehyde, infused with 20% sucrose overnight, rinsed in PBS, embedded in OCT, and cryosectioned. All sections were immediately fixed with 4% paraformaldehyde, permeabilized with pepsin, blocked with ISH solution (Dako, Carpinteria, CA), and incubated with RNA probes (100 ng/ml) overnight at 55°C. After washing twice in 2× SSC and then once in TNE buffer [10 mM Tris-HCl (pH 7.5), 500 mM NaCl, and 1 mM EDTA], sections were incubated at 37°C with RNase mixture (Ambion, Austin, TX) diluted 1:35 in TNE. Slides were stringently washed twice in 2× SSC/50% deionized formamide (American Bioanalytical, Natick, MA) and then once with 0.1× SSC at 55°C. Before immunodetection, tissues were treated with peroxidase blocking reagent (DAKO) and blocked with 1% blocking reagent (Roche; DIG Nucleic Acid Detection kit) containing purified, nonspecific rabbit immunoglobulins (DAKO). For signal amplification, a horseradish peroxidase-rabbit anti-DIG antibody (DAKO) was used to catalyze the deposition of Biotin-Tyramide (GenPoint kit; DAKO). Further amplification was achieved by adding horseradish peroxidase-rabbit anti-biotin (DAKO), biotin tyramide, and then alkaline phosphatase rabbit anti-biotin (DAKO). Signal was detected with the alkaline phosphatase substrate Fast Red TR/Napthol AS-MX (Sigma Chemical Co., St. Louis, MO). All sections were exposed for 10 min. Cells were counterstained with hematoxylin and mounted with Crystal/Mount (Biomeda, Foster City, CA).

Results

Identification of Cell Surface *TEM*s. Using SAGE technology, we previously identified partial cDNAs corresponding to several novel genes (*TEM1–8*) that were expressed in tumor endothelial cells (6). Because many cell surface proteins have their signal sequences at the NH_2 terminus, it was important to obtain full-length clones to determine which of these would likely be located on the cell surface. The 15-bp SAGE tags from the eight most abundantly expressed novel *TEM*s were used to identify corresponding 3′ EST clones, and then a combination of *in silico* cDNA walking and 5′ RACE was used to derive sequences covering the entire coding region. Four TEMs (TEM1, TEM5, TEM7, and TEM8) had sequence characteristics, including signal recognition sequences and transmembrane domains, indicative of cell surface proteins (Fig. 1 and Table 1). Additionally, the presence of the signal peptides confirmed that we had identified the complete open reading frames of these genes. Each of these four TEMs was unique with respect to each other and to other proteins in the databases.

TEM1 was predicted to encode a type I transmembrane protein of 757 amino acids (Table 1). The majority (685 amino acids) of the sequence was predicted to be extracellular, with only a short COOH-terminal cytoplasmic tail. A homology search revealed that the extracellular region of TEM1 has three EGF-like domains, as well as a C-lectin-like carbohydrate recognition domain with similarity to thrombomodulin (Fig. 1). In addition, amino acids 164–230 bear weak homology to a Sushi/SCR/CCP domain.

TEM5 is predicted to encode a seven-pass transmembrane protein of 1331 amino acids (Table 1). The hydrophobic domains lie within a 300-amino acid region that shares homology with seven-pass transmembrane proteins of the secretin family (class II) of GPCRs (13), suggesting that TEM5 also may be a GPCR. In the NH_2-terminal extracellular region, TEM5 contains four simple LRRs, one LRR of the COOH-terminal type, one immunoglobulin-type domain, and a hormone-receptor domain (Fig. 1). The 300-amino acid region containing the LRRs shares homology with the membrane glycoprotein, known as LIG-1 (14), and the secreted SLIT proteins (15). In the extracellular region immediately adjacent to the first transmembrane domain, TEM5 contains a putative GPCR proteolysis site (16) domain typical of class II family members and required for endogenous proteolysis (Ref. 17; Fig. 1). Within its seven-pass transmembrane region, TEM5 is most similar to the cadherin-related Celsr1 proteins (18–20) and members of the calcium-independent α-latrotoxin receptor family (21). Taken together, these data suggest that TEM5 is likely to be a novel member of the GPCR superfamily involved in transmitting signals across the cell membrane, although its function as a G-protein coupled receptor remains to be proven.

Similar to *TEM1*, *TEM7* was found to encode a type I transmembrane protein with a large extracellular domain, a hydrophobic transmembrane domain, and a short cytoplasmic tail (Fig. 1 and Table 1). The extracellular region of TEM7 contains a plexin-like domain and has weak homology to the ECM protein nidogen. The function of these domains, which are usually found in secreted and extracellular matrix molecules, is unknown. Interestingly, during the course of performing 5′ RACE to extend the sequence identified previously by the *TEM3* SAGE tag, we obtained sequences of the gene we had identified previously as *TEM7*. Further investigation revealed that *TEM3* and *TEM7* represent alternative transcripts of the same gene,

Table 1 *Structural characteristics of TEMs*

Name	Accession no.	Signal peptide	TM domains	AA[a] length
Human				
TEM1	AF279142	Y	1	757
TEM2	AF279143	N	0	278
TEM3[b]	AF378753	Y	1	500
TEM4	AF378754	N	0	1510
TEM5	AF378755	Y	7	1331
TEM6	AF378756	N	0	261
TEM7	AF279144	Y	1	500
TEM7R	AF378757	Y	1	529
TEM8	AF279145	Y	1	564
Mouse				
mTEM1	AF378758	Y	1	765
mTEM5	AF378759	Y	7	1329
mTEM7	AF378760	Y	1	500
mTEM7R	AF378761	Y	1	530
mTEM8	AF378762	Y	1	562

[a] AA, amino acid.
[b] *TEM3* encodes an alternate transcript of *TEM7*.

Table 2 *In situ hybridization of adult mouse tissues*

		Normal adult tissues[b]											Tumors	
Name	% iden[a]	Ad	Br	H	I	Ki-C	Ki-M	Li	Lg	M	P	Sp	St	B16	HCT
mTEM1	77	+	+	+	+	−	−	−	+	+	+	−	−	+++	+++
mTEM5	87	−	+	+	+	−	−	−	+	+	+	−	−	+++[c]	+++
mTEM7	81	−	+++[d]	−	−	−	−	−	−	−	−	−	−	−	−
mTEM7R	91	−	+[e]	+	+	−	−	+	+++	+++	+	+	−	ND[f]	+++
mTEM8	96	−	+	+	+	−	−	−	+	+	+	−	−	+++[c]	+++
VEGFR	N/A	+++	++	+++	+++	+++	+++	+++	+++	+++	+++	+++	+++	+++	+++

[a] The percentage of amino acid identity to homologous human TEMs.
[b] −, no endothelial cell staining detected; +, weak positive staining of endothelial cells; ++, moderate staining of endothelial cells; +++, strong staining of endothelial cells. Ad, adrenal gland; B, brain; H, heart; I, intestine; Ki-C, kidney cortex; Ki-M, kidney medulla; Li, liver; Lg, lung; M, skeletal muscle; P, pancreas; Sp, spleen; St, stomach; HCT, HCT116 human colon carcinoma xenograft; B16, B16 mouse melanoma tumor.
[c] Endothelial cells were strongly positive; some B16 tumor cells were also weakly positive.
[d] Strong staining localized to the Purkinje cells of the cerebellum and some neuronal cells.
[e] Weak staining localized primarily to Purkinje cells.
[f] ND, not determined.

with the differences simply attributable to the use of alternative polyadenylation sites. Because the predicted open reading frame of the two transcripts was the identical 500-amino acid protein, we refer to the gene product of both as *TEM7*.

Finally, completion of the *TEM8* sequence also revealed a type I transmembrane protein (Fig. 1 and Table 1), 564 amino acids in length. The 220-amino acid cytoplasmic tail of TEM8 is much larger than that of the other cell surface TEMs. In the extracellular region, TEM8 was found to contain a vWF A domain containing a metal ion-dependent adhesion motif (MIDAS; Refs. 22 and 23). The vWF A domain is also known as an I-domain when present in integrins (24). The TEM8 domain is most similar to that of αD integrin, which has been shown to interact with vascular cell adhesion molecule via its I-domain during leukocyte trafficking (25).

Identification of Mouse *TEM*s. We next searched for the mouse orthologues of the human cell surface *TEM*s. In all four cases, it was possible to identify highly related mouse ESTs in extant databases and, as with the human *TEM*s, a combination of *in silico* cDNA walking, and both 3′ and 5′ RACE were used to derive sequences covering the entire coding region (Table 1). All four mouse TEMs (mTEM1, mTEM5, mTEM7, and mTEM8) shared the same domain structures as their human counterparts. The hydrophobicity plots were also similar to those observed for the human genes, with putative signal peptides at the start and transmembrane domains present in the same relative positions (data not shown). Although TEM1 was the least similar overall, both the NH_2-terminal C-lectin like domain of the extracellular region as well as its COOH-terminal transmembrane and cytoplasmic tail were >90% identical. A highly conserved rat EST (GenBank accession number BF388781) was also found to extend across the COOH-terminal region and revealed that the last 20 amino acids of the cytoplasmic tail are 100% identical in mouse, human, and rat. Although the function of the COOH terminus is unknown, it includes a consensus sequence for binding of some PDZ domains (26). TEM5 was most homologous through its LRR repeats and transmembrane domains, suggesting that these regions might play a conserved functional role. TEM8 was the most highly conserved overall, sharing 96% amino acid identity between mouse and human (Table 2). The high degree of identity between the mouse and human TEMs and their functional conservation in tumor angiogenesis (described below) suggest that they are likely to be orthologues.

Identification of *mTEM7R* and *TEM7R*. During the course of searching for a *TEM7* homologue in mouse, we identified an apparent mouse paralogue (*mTEM7R*), indicating that *TEM7* is part of a family comprised of at least two members. On the basis of this observation, we went on to discover a human sequence highly related to *mTEM7R*, which we designated *TEM7R* (Table 1). Interestingly, all four sequences (TEM7, mTEM7, TEM7R, and mTEM7R) shared significant homology over 270 amino acids of their putative extracellular domains, although the most NH_2-terminal regions were divergent (data not shown). The plexin-like domains lie within the conserved NH_2-terminal region. The cytoplasmic tail is also conserved but is unrelated to other known proteins. Importantly, TEM7R and mTEM7R both contain putative signal peptides and transmembrane regions in the same relative positions as TEM7.

***TEM*s in Tumor Angiogenesis.** To confirm the mRNA localization of the full-length cell surface *TEM*s in tumor endothelium and to explore the expression of *TEM7R*, we modified our nonradioactive *in situ* hybridization technique to achieve increased sensitivity (see "Materials and Methods" for details). Acquisition of the complete sequences for *TEM1*, *TEM5*, *TEM7*, *TEM7R*, and *TEM8* allowed us to compare multiple RNA probes, further improving the sensitivity of the *in situ* hybridization protocol. As controls, various endothelial cell markers, such as *vWF*, *CD31* (*PECAM*), *VE-cadherin*, *P1H12*, and *VEGFR2*, were used. Classic endothelial cell markers such as *vWF*, *CD31* and *VE-cadherin* were detected predominantly in the larger vessels. Although *P1H12* detected many microcapillaries, *VEGFR2* was the best pan endothelial marker and appeared to detect most microvessels in addition to the larger vessels. Thus, we chose to use *VEGFR2* as our positive control.

The *in situ* hybridization analysis of human colorectal cancer demonstrated that all four cell surface *TEM*s and *TEM7R* were expressed clearly in the endothelial cells of the tumor stroma but not in the endothelial cells of normal colonic tissue (Fig. 2). Interestingly, all *TEM*s demonstrated local regions of intense staining throughout the stromal compartment. The microcapillaries were likely to account for much of the staining, because vascular casting techniques have demonstrated the presence of a virtually continuous layer of anastomatizing vessels throughout the lamina propria in advanced colorectal cancers (27). However, we cannot rule out the possibility that other stromal cells (*e.g.*, fibroblasts) also expressed these *TEM*s, although staining was not observed in normal colonic mucosa (Fig. 2).

To analyze expression of *mTEM*s in murine tumors, B16 mouse melanoma or HCT116 human colon carcinoma cells were implanted s.c. into mice and used for *in situ* hybridization studies. As shown in Fig. 3 and Table 2, *mTEM1*, *mTEM5*, and *mTEM8* were abundantly expressed in vessels infiltrating both B16 and HCT116 tumors. Unexpectedly, we were unable to detect significant levels of *mTEM7* in vessels of either tumor type, despite the fact that its human counterpart, *TEM7*, was abundantly expressed in human tumor endothelial cells when assessed with the same *in situ* hybridization methods (Fig. 2 and data not shown). Importantly, the lack of *mTEM7* signal in tumor vessels was unlikely to be attributable to technical problems, because other cell types were clearly positive (see below). In contrast

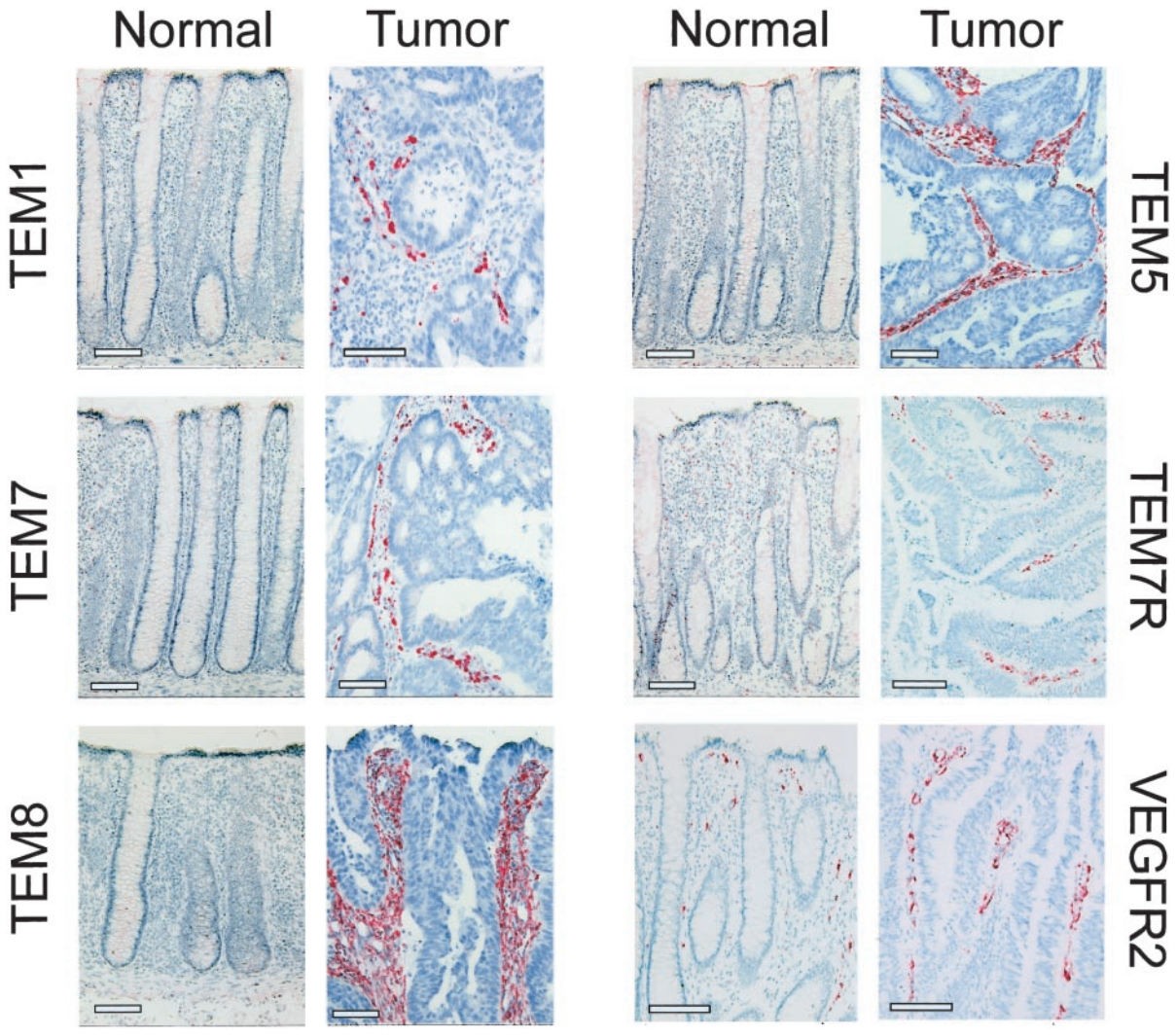

Fig. 2. *TEM*s in normal human colon and colorectal carcinoma tissues. Expression of *TEM1*, *TEM5*, *TEM7*, *TEM7R*, and *TEM8* was assessed by *in situ* hybridization. *VEGFR2* was used as a positive control for endothelial cells. Expression of all five *TEM*s (*red* stain) was highly specific to tumor endothelial cells and was not detected in the endothelial cells of the normal colonic mucosa. The *faint red* extracellular staining around the crypts represents nonspecific binding of the *in situ* hybridization reagents to the mucous. Sections were counterstained with hematoxylin (*blue*). *Bars*, 100 μm.

to *mTEM7*, expression of *mTEM7R* was readily detectable in tumor endothelium (data not shown).

***TEM*s in Normal Adult Tissue.** We next assayed expression of *mTEM*s in various normal adult tissues by *in situ* hybridization. *VEGFR2* was readily detected in vessels of every tissue analyzed, including adrenal gland, brain, heart, intestine, kidney (cortex and medulla), liver, lung, skeletal muscle, pancreas, spleen, and stomach (Table 2). In sharp contrast, *mTEM1*, *mTEM5*, and *mTEM8* were either undetectable, as in kidney and liver (Figs. 4 and 5), or were only detected in a small proportion of the vessels, as in the heart (Fig. 4). These rare *TEM*-expressing vessels may represent a low but significant level of ongoing angiogenesis in the adult, because 3- and 9-month-old mice both showed the same pattern. Although negative *in situ* hybridization results should be interpreted with caution, tumors were always included as a positive control in these experiments and always demonstrated strong staining for *mTEM1*, *mTEM5*, and *mTEM8*.

The analyses of normal mouse tissues also yielded important information about *mTEM7* and *mTEM7R*. RNA for *mTEM7*, although largely undetectable in mouse tissues or tumors, was abundantly expressed in Purkinje cells of the mouse cerebellum (data not shown). Unlike the other cell surface *TEM*s, *mTEM7R* was expressed at high levels not only in tumor endothelium but also in vessels of some normal tissues, such as the muscle and lung (Table 2). Thus, in mice neither *mTEM7* nor *mTEM7R* expression patterns accurately recapitulated that of *TEM7* in humans.

Expression of *TEM*s during Development. Previous analyses of human *TEM*s have suggested that tumor angiogenesis shares some features with normal neoangiogenic processes, such as those found in wound healing and the corpus luteum (6). To determine whether *TEM*s were also up-regulated in endothelium during normal development, *in situ* hybridizations were performed on developing mouse embryos. At E15.5, *mTEM1*, *mTEM5*, and *mTEM8* were all abundantly expressed in endothelial cells of the liver. In contrast, in the adult liver, expression of these three *mTEM*s was undetectable (Fig. 5). Similarly, *mTEM* expression was high in the endothelium of embryonic brain tissue, whereas staining in the corresponding adult tissue was weak or absent (Table 2 and data not shown). Thus, the murine *TEM*s were expressed in various neoangiogenic states, whether normal or pathological.

Discussion

The extent of overlap between tumor angiogenesis in rodents and humans is unclear. Although some cell surface proteins have been identified as important regulators of angiogenesis in both in mice and men

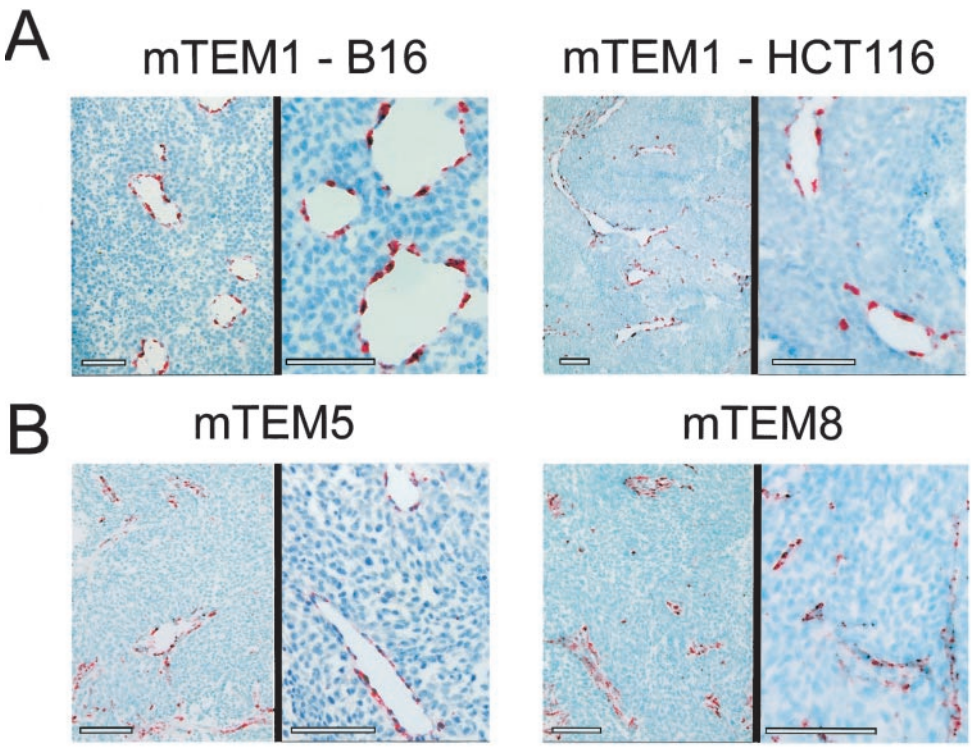

Fig. 3. *mTEM*s in mouse tumors. *A*, expression of *mTEM1* in B16 melanoma tumor endothelial cells and HCT116 colon tumor endothelial cells was assessed by *in situ* hybridization. *mTEM1* staining is specific to the endothelial cells of the vessels and microcapillaries, as shown in a low-power field (*left*) and a high-power field (*right*). *B*, expression of *mTEM5* and *mTEM8* in HCT116 tumor endothelial cells. Note that staining is localized to the endothelial cells. *Bars*, 100 μm.

(*e.g.*, *VEGFR1*, *VEGFR2*, *Tie-1*, and *Tie-2*), others may be more species specific. For example, in humans *Thy-1* appears to be predominantly expressed in angiogenic vessels, whereas in mice, its expression is most obvious in hematopoietic cells, especially T-lymphocytes (6, 28, 29). The pronounced effects of angiogenesis inhibitors observed in rodent models have, to date, been much less impressive in humans (30). This could be related to the degree of angiogenesis in humans *versus* mice, species-specific differences in drug sensitivity and tolerance, or species-specific expression of genes regulating tumor angiogenesis.

Here we report the complete coding sequences of four abundant and

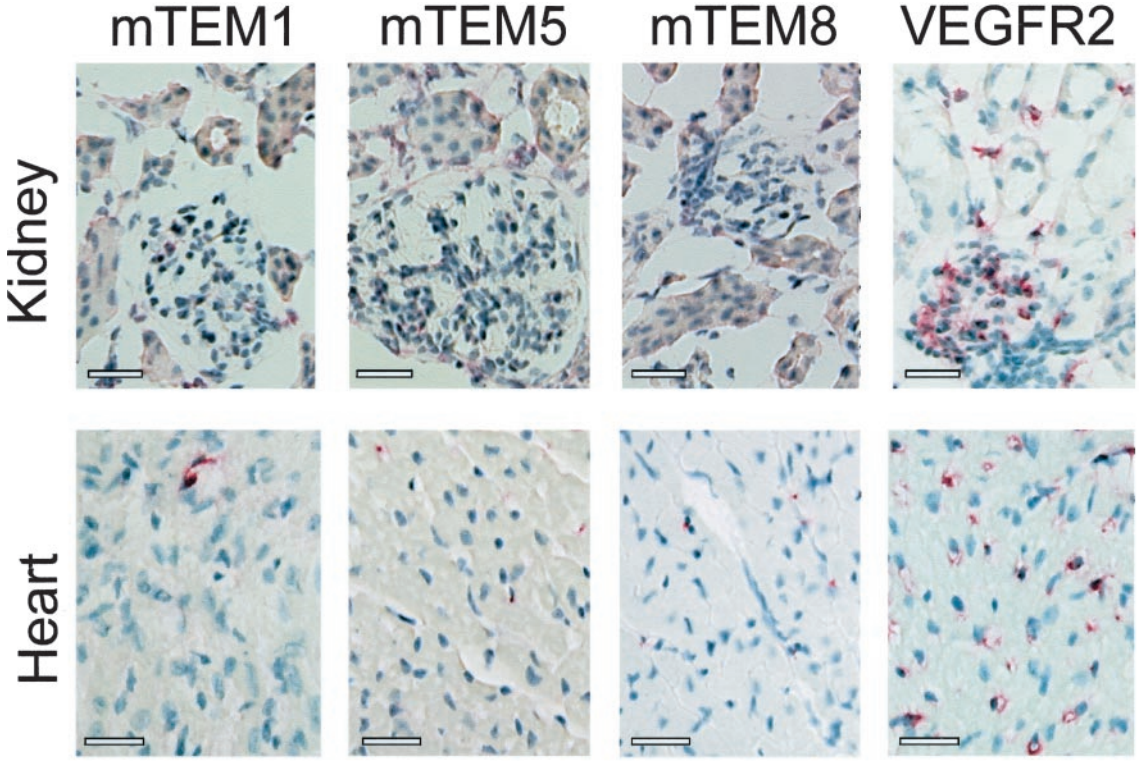

Fig. 4. *mTEM*s in adult mouse tissues. Expression of *mTEM1*, *mTEM5*, and *mTEM8* was examined by *in situ* hybridization in adult mouse tissues. *mTEM* expression was undetectable in kidney (glomeruli and tubules), whereas *VEGFR2* expression (*red*) was easily detected in the endothelial cells of these tissues. In the heart, expression of *mTEM1*, *mTEM5*, and *mTEM8* could be detected in occasional endothelial cells, as compared with the widespread expression of *VEGFR2*. *Bars*, 25 μm.

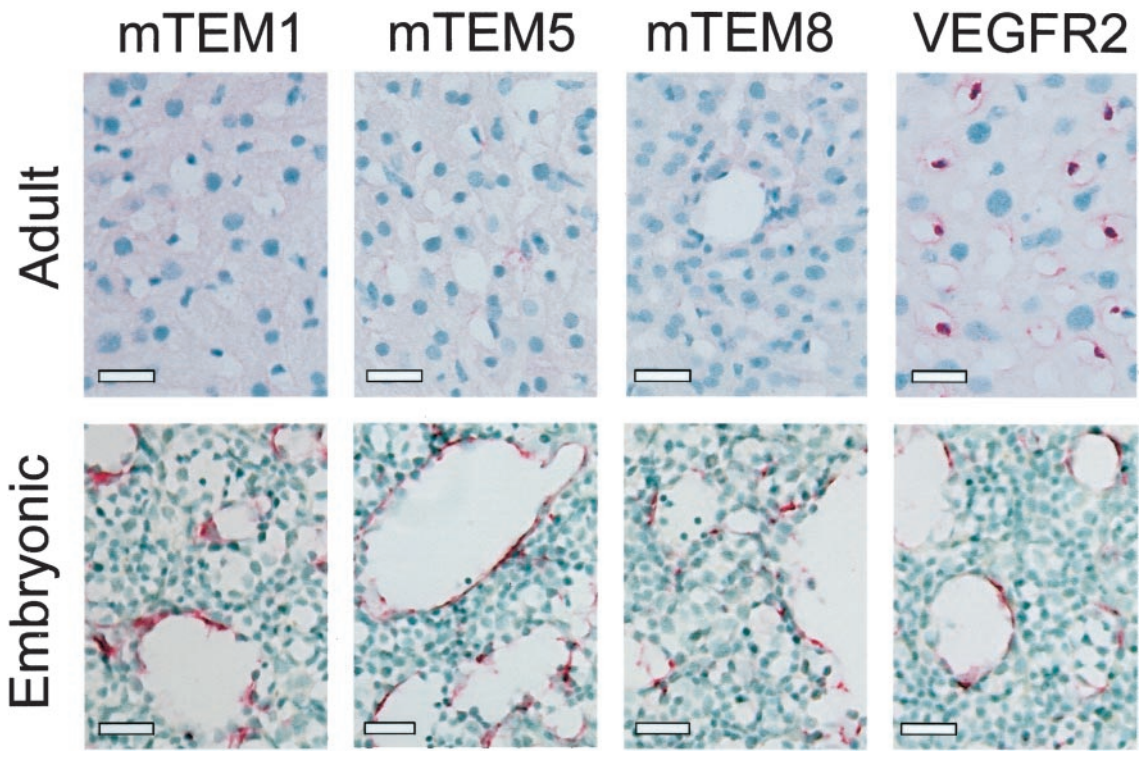

Fig. 5. *mTEM*s in embryonic and adult liver. Expression of *mTEM1*, *mTEM5*, and *mTEM8* was examined by *in situ* hybridization in adult and embryonic mouse liver. Expression was undetectable in the adult liver endothelial cells, but all three *mTEM*s were strongly expressed in embryonic liver endothelial cells, at levels comparable with that of *VEGFR2*. *Bars*, 25 μm.

differentially expressed *TEM*s predicted to contain hydrophobic transmembrane domains. The mouse TEM counterparts we identified show a high level of identity with their respective human TEMs, ranging from 77 to 96%. These similarities and conserved expression patterns suggest that we have cloned the mouse orthologues of human *TEM1*, *TEM5*, *TEM7*, *TEM7R*, and *TEM8*. Currently, each of the cell surface *TEMs* has unique features that make it attractive for further investigation.

TEM1 was the most differentially expressed *TEM* identified previously in our original SAGE analysis (6). The recent purification of endosialin, a glycoprotein recognized by the FB5 antibody, revealed an amino acid sequence identical to TEM1 (31). Immunostaining with FB5 was specific for tumor microvessels, because a panel of normal tissues was negative for TEM1/endosialin immunoreactivity (32). Thus, TEM1/endosialin appears to be differentially expressed at both the mRNA and protein levels. Interestingly, Rettig *et al.* (32) reported that radiolabeled FB5 was rapidly internalized into TEM1/endosialin expressing endothelial cells. If this is the case, it may be possible to deliver compounds to TEM1/endosialin-expressing cells for selective uptake.

TEM5 appears to be a member of the class II GPCR family. GPCRs have a history of being excellent drug targets because their natural ligands can often be mimicked for agonistic or antagonistic purposes (33). Other class II GPCRs bind peptide ligands, such as secretin, calcitonin, and vasoactive intestinal peptide, and activate adenylyl cyclase and inositol phosphate signaling cascades (34, 35). These findings tentatively suggest that TEM5 may also transmit signals into the cell, but the signaling partners of TEM5 remain to be determined.

In the current study, we found that the human *TEM7* gene encodes two transcripts that differed only in the length of their 3′ untranslated region. The murine and human TEM7 proteins are over 80% conserved, but despite these similarities, transcripts of *mTEM7* were not detectable by *in situ* hybridization in mouse tumors (Table 2 and data not shown). There are several possible explanations for this. *mTEM7*, through the course of evolution, could have acquired different functions than human *TEM7*. Support for this possibility comes from the specific expression of *mTEM7* in Purkinje cells of the mouse brain. Alternatively, there may exist an as yet unidentified mouse counterpart with greater homology than *mTEM7* or *mTEM7R*. Although we cannot formally rule out this possibility, it seems unlikely because we were unable to identify more highly related homologues in EST or mouse genomic databases. The lack of expression of *mTEM7* in mouse tumor vessels highlights potentially important differences between mouse and human tumor angiogenesis.

TEM8 is the most highly conserved cell surface TEM, with 96% amino acid identity between the human and mouse proteins. The large cytoplasmic tail of both the human and mouse TEM8 proteins share at least seven potential phosphorylation sites, supporting the hypothesis that TEM8 is involved in transmitting signals into the cell. The expression pattern of *TEM8* was especially intriguing in that it is the only human *TEM* characterized thus far that shows no detectable mRNA expression in either the corpus luteum or healing wounds, suggesting that this gene may be highly specific to tumor angiogenesis and not required for "normal" adult angiogenesis (6). From a clinical point of view, this could be important in designing gene-targeting strategies with the fewest cross-reactivities.

The fact that *mTEM1*, *mTEM5*, and *mTEM8* were present in the vasculature of developing embryos as well as in the vessels of transplanted syngeneic and human tumors is consistent with the idea that they are markers of neoangiogenesis and not limited to tumor angiogenesis. The data further support the hypothesis that tumor endothelium exploits many of the same genes used by normal developing endothelium.

Our detailed comparison of *TEM* expression in human and rodent angiogenesis is provocative in that it demonstrates that three of the four cell surface *TEM*s identified in humans are also expressed in

mouse tumors. The uniqueness of these *TEM*s was emphasized by comparison with *VEGFR2*, believed to be one of the most specific markers for tumor angiogenesis available. We found that *VEGFR2* transcripts were expressed in the endothelium of all normal adult tissues studied, whereas expression of the cell surface *TEM*s was largely restricted to the vasculature of tumors in adult animals. The high degree of sequence conservation of these *TEM*s, in combination with their restricted expression patterns, suggests that they may be critical regulators of angiogenesis. Continued investigation of all four cell surface *TEM*s should foster better understanding of the mechanisms of tumor angiogenesis and encourage rational design of interventional strategies.

Acknowledgments

We thank L. Meszler (Johns Hopkins Oncology Cell Imaging Facility) for expert help with the microscopic imaging. We thank members of the Kinzler/Vogelstein laboratory for helpful discussion and critical comments.

References

1. Folkman, J. Tumor Angiogenesis. *In:* J. F. Holland and E. Frei (eds.), Cancer Medicine, Ed. 5, pp. 132–152. Hamilton, Ontario, Canada: B. C. Decker, 2000.
2. Kerbel, R. S. Tumor angiogenesis: past, present and the near future. Carcinogenesis (Lond.), *21:* 505–515, 2000.
3. Jain, R. K. Delivery of molecular and cellular medicine to solid tumors. Adv. Drug Delivery Rev., *46:* 149–168, 2001.
4. Kerbel, R. S. Inhibition of tumor angiogenesis as a strategy to circumvent acquired resistance to anti-cancer therapeutic agents. Bioessays, *13:* 31–36, 1991.
5. Boehm, T., Folkman, J., Browder, T., and O'Reilly, M. S. Antiangiogenic therapy of experimental cancer does not induce acquired drug resistance. Nature (Lond.), *390:* 404–407, 1997.
6. St. Croix, B., Rago, C., Velculescu, V., Traverso, G., Romans, K. E., Montgomery, E., Lal, A., Riggins, G. J., Lengauer, C., Vogelstein, B., and Kinzler, K. W. Genes expressed in human tumor endothelium. Science (Wash. DC), *289:* 1197–1202, 2000.
7. Thompson, J. D., Higgins, D. G., and Gibson, T. J. CLUSTAL W: improving the sensitivity of progressive multiple sequence alignment through sequence weighting, position-specific gap penalties and weight matrix choice. Nucleic Acids Res., *22:* 4673–4680, 1994.
8. Cserzo, M., Wallin, E., Simon, I., von Heijne, G., and Elofsson, A. Prediction of transmembrane α-helices in prokaryotic membrane proteins: the dense alignment surface method. Protein Eng., *10:* 673–676, 1997.
9. Nielsen, H., Engelbrecht, J., Brunak, S., and von Heijne, G. Identification of prokaryotic and eukaryotic signal peptides and prediction of their cleavage sites. Protein Eng., *10:* 1–6, 1997.
10. Schultz, J., Milpetz, F., Bork, P., and Ponting, C. P. SMART, a simple modular architecture research tool: identification of signaling domains. Proc. Natl. Acad. Sci. USA, *95:* 5857–5864, 1998.
11. Bateman, A., Birney, E., Durbin, R., Eddy, S. R., Howe, K. L., and Sonnhammer, E. L. The Pfam protein families database. Nucleic Acids Res., *28:* 263–266, 2000.
12. Yaffe, M. B., Leparc, G. G., Lai, J., Obata, T., Volinia, S., and Cantley, L. C. A motif-based profile scanning approach for genome-wide prediction of signaling pathways. Nat. Biotechnol., *19:* 348–353, 2001.
13. Laburthe, M., Couvineau, A., Gaudin, P., Maoret, J. J., Rouyer-Fessard, C., and Nicole, P. Receptors for VIP, PACAP, secretin, GRF, glucagon, GLP-1, and other members of their new family of G protein-linked receptors: structure-function relationship with special reference to the human VIP-1 receptor. Ann. NY Acad. Sci., *805:* 94–109; discussion 110–111, 1996.
14. Suzuki, Y., Sato, N., Tohyama, M., Wanaka, A., and Takagi, T. cDNA cloning of a novel membrane glycoprotein that is expressed specifically in glial cells in the mouse brain. LIG-1, a protein with leucine-rich repeats and immunoglobulin-like domains. J. Biol. Chem., *271:* 22522–22527, 1996.
15. Yuan, W., Zhou, L., Chen, J. H., Wu, J. Y., Rao, Y., and Ornitz, D. M. The mouse SLIT family: secreted ligands for ROBO expressed in patterns that suggest a role in morphogenesis and axon guidance. Dev. Biol., *212:* 290–306, 1999.
16. Krasnoperov, V., Bittner, M. A., Holz, R. W., Chepurny, O., and Petrenko, A. G. Structural requirements for α-latrotoxin binding and α-latrotoxin-stimulated secretion. A study with calcium-independent receptor of α-latrotoxin (CIRL) deletion mutants. J. Biol. Chem., *274:* 3590–3596, 1999.
17. Sugita, S., Ichtchenko, K., Khvotchev, M., and Sudhof, T. C. α-Latrotoxin receptor CIRL/latrophilin 1 (CL1) defines an unusual family of ubiquitous G-protein-linked receptors. G-protein coupling not required for triggering exocytosis. J. Biol. Chem., *273:* 32715–32724, 1998.
18. Usui, T., Shima, Y., Shimada, Y., Hirano, S., Burgess, R. W., Schwarz, T. L., Takeichi, M., and Uemura, T. Flamingo, a seven-pass transmembrane cadherin, regulates planar cell polarity under the control of Frizzled. Cell, *98:* 585–595, 1999.
19. Nakayama, M., Nakajima, D., Nagase, T., Nomura, N., Seki, N., and Ohara, O. Identification of high-molecular-weight proteins with multiple EGF-like motifs by motif-trap screening. Genomics, *51:* 27–34, 1998.
20. Hadjantonakis, A. K., Sheward, W. J., Harmar, A. J., de Galan, L., Hoovers, J. M., and Little, P. F. *Celsr1,* a neural-specific gene encoding an unusual seven-pass transmembrane receptor, maps to mouse chromosome 15 and human chromosome 22qter. Genomics, *45:* 97–104, 1997.
21. Ichtchenko, K., Bittner, M. A., Krasnoperov, V., Little, A. R., Chepurny, O., Holz, R. W., and Petrenko, A. G. A novel ubiquitously expressed α-latrotoxin receptor is a member of the CIRL family of G-protein-coupled receptors. J. Biol. Chem., *274:* 5491–5498, 1999.
22. Colombatti, A., and Bonaldo, P. The superfamily of proteins with von Willebrand factor type A-like domains: one theme common to components of extracellular matrix, hemostasis, cellular adhesion, and defense mechanisms. Blood, *77:* 2305–2315, 1991.
23. Lee, J. O., Rieu, P., Arnaout, M. A., and Liddington, R. Crystal structure of the A domain from the α subunit of integrin CR3 (CD11b/CD18). Cell, *80:* 631–638, 1995.
24. Dickeson, S. K., and Santoro, S. A. Ligand recognition by the I domain-containing integrins. Cell. Mol. Life Sci., *54:* 556–566, 1998.
25. Van der Vieren, M., Crowe, D. T., Hoekstra, D., Vazeux, R., Hoffman, P. A., Grayson, M. H., Bochner, B. S., Gallatin, W. M., and Staunton, D. E. The leukocyte integrin $\alpha D\beta 2$ binds VCAM-1: evidence for a binding interface between I domain and VCAM-1. J. Immunol., *163:* 1984–1990, 1999.
26. Songyang, Z., Fanning, A. S., Fu, C., Xu, J., Marfatia, S. M., Chishti, A. H., Crompton, A., Chan, A. C., Anderson, J. M., and Cantley, L. C. Recognition of unique carboxyl-terminal motifs by distinct PDZ domains. Science (Wash. DC), *275:* 73–77, 1997.
27. Skinner, S. A., Frydman, G. M., and O'Brien, P. E. Microvascular structure of benign and malignant tumors of the colon in humans. Dig. Dis. Sci., *40:* 373–384, 1995.
28. Lee, W. S., Jain, M. K., Arkonac, B. M., Zhang, D., Shaw, S. Y., Kashiki, S., Maemura, K., Lee, S. L., Hollenberg, N. K., Lee, M. E., and Haber, E. Thy-1, a novel marker for angiogenesis upregulated by inflammatory cytokines. Circ. Res., *82:* 845–851, 1998.
29. Risau, W. Angiogenesis is coming of age. Circ. Res., *82:* 926–928, 1998.
30. Westphal, J. R., Ruiter, D. J., and De Waal, R. M. Anti-angiogenic treatment of human cancer: pitfalls and promises. Int. J. Cancer, *86:* 870–873, 2000.
31. Christian, S., Ahorn, H., Koehler, A., Eisenhaber, F., Rodi, H. P., Garin-Chesa, P., Park, J. E., Rettig, W. J., and Lenter, M. C. Molecular cloning and characterization of endosialin, a C-type lectin-like cell surface receptor of tumor endothelium. J. Biol. Chem., *276:* 7408–7414, 2000.
32. Rettig, W. J., Garin-Chesa, P., Healey, J. H., Su, S. L., Jaffe, E. A., and Old, L. J. Identification of endosialin, a cell surface glycoprotein of vascular endothelial cells in human cancer. Proc. Natl. Acad. Sci. USA, *89:* 10832–10836, 1992.
33. Wilson, S., Bergsma, D. J., Chambers, J. K., Muir, A. I., Fantom, K. G., Ellis, C., Murdock, P. R., Herrity, N. C., and Stadel, J. M. Orphan G-protein-coupled receptors: the next generation of drug targets? Br. J. Pharmacol., *125:* 1387–1392, 1998.
34. Gether, U. Uncovering molecular mechanisms involved in activation of G protein-coupled receptors. Endocr. Rev., *21:* 90–113, 2000.
35. Schoneberg, T., Schultz, G., and Gudermann, T. Structural basis of G protein-coupled receptor function. Mol. Cell. Endocrinol., *151:* 181–193, 1999.